NOTES AND CORRESPONDENCE

Parameterization of Mesoscale Eddies as Inferred from a High-Resolution Circulation Model

NILS H. RIX AND JÜRGEN WILLEBRAND

Institut für Meereskunde an der Universität Kiel, Kiel, Germany

15 May 1995 and 18 October 1995

ABSTRACT

The compatibility of the Gent and McWilliams thickness mixing parameterization with perturbation thickness fluxes evaluated from eddy-resolving North Atlantic model results is investigated. After extensive spatial and temporal averaging, a linear correlation between the parameterized fluxes and those calculated directly from model fluctuations in the subtropics could be found. A direct estimate of a constant mixing parameter κ could be inferred in the order of 1.0×10^7 cm^2 s^{-1}.

1. Introduction

An eddy mixing parameterization based on the concept of isopycnal layer diffusion was proposed by Gent and McWilliams (1990, hereafter GM90) and revisited by Gent et al. (1995). The latter show that the parameterization can be viewed as a quasi-adiabatic advection of a mean tracer field by an eddy-induced velocity. This velocity acts in addition to the Eulerian mean advection velocity, which is normally used in the tracer equations, thus constituting an effective transport velocity (e.g., Rhines 1986). The use of the effective transport velocity in non-eddy-resolving calculations can be considered as a step toward a better representation of the effect of mesoscale eddies on the large-scale flow.

The new parameterization has been implemented in several numerical experiments, in combination with the standard form for isopycnal diffusion (Redi 1982). Danabasoglu et al. (1994) report clear improvements with the new scheme. In particular, they obtained a sharper thermocline and cooler abyssal ocean and a larger meridional extent of the overturning cell with a strengthened poleward heatflux in the North Atlantic. They also found a confinement of deep convection regions to a more realistic extent. Böning et al. (1995) report a reduction of spurious upwelling in the western boundary region that leads to a more realistic latitudinal structure and magnitude of the poleward heat transport. This is accomplished due to the reduction of unphysical horizontal diffusion, which causes a shortcut of the meridional overturning cell.

While these results from coarse-resolution models are encouraging, it remains to be shown that the mean effect of mesoscale eddies on the oceanic temperature and salinity distribution indeed is compatible with the GM90 parameterization. As direct measurements of eddy-induced fluxes in the ocean are virtually nonexistent, it seems sensible to utilize data from experiments with high-resolution circulation models where the eddies are explicitly resolved. These models have meanwhile achieved a considerable degree of realism and, in particular, simulate the amplitude and regional distribution of mesoscale eddies reasonably well, at least in low latitudes. Provided that the model statistics are sufficiently accurate, such model data in principle allow evaluation of all relevant fluxes so that the proposed mixing parameterization can be tested directly, as opposed to the indirect test in coarse-resolution models.

In this note we report an attempt to directly verify the GM90 parameterization with results obtained from the WOCE Community Modelling Effort in Kiel (cf. Böning and Herrmann 1994). In the next section we derive a simple method to calculate the relevant eddy-induced transport velocity from model results and to compare it with the GM90 parameterization. After a short discussion of the high-resolution model experiments used for this study, results of the comparison are presented and discussed in the concluding section.

2. Method

A comprehensive derivation and discussion of the mixing effects induced by mesoscale eddies can be

Corresponding author address: Nils H. Rix, Department of Theoretical Oceanography, Institut für Meereskunde an der Universität Kiel, Düsternbrookerweg 20, Kiel 24116, Germany.
e-mail: nrix@ifm.uni-kiel.de

found in McDougall (1991). GM90 propose a subgrid-scale parameterization for such effects that can be viewed as an eddy-induced, quasi-adiabatic advection of layer thickness (Gent et al. 1995). It may just be stated here that a mean tracer field is advected along isopycnals by an effective transport velocity

$$\mathbf{U} = \bar{\mathbf{u}} + \frac{\overline{h'_\rho \mathbf{u}'}}{\bar{h}_\rho} = \bar{\mathbf{u}} + \boldsymbol{u}_B$$

(h_ρ is the isopycnal layer thickness and the overbar denotes an average over the eddy field), which is the sum of the Eulerian mean velocity $\bar{u}$ and a turbulent advection of layer thickness $\boldsymbol{u}_B$, which is termed bolus velocity by McDougall (1991).

Layer thickness is not a natural variable in a z-coordinate model formulation, and therefore the perturbation thickness fluxes have to be calculated from eddy temperature and salinity fluxes. The eddy-induced elevation of a density surface h' is related to density perturbation by

$$h' \approx -\frac{\rho'}{\bar{\rho}_z}.$$

The layer thickness perturbation then is

$$h'_\rho \approx \frac{1}{\bar{\rho}_z} h'_z = -\frac{1}{\bar{\rho}_z}\frac{\partial}{\partial z}\left(\frac{\rho'}{\bar{\rho}_z}\right).$$

This leads to a first-order approximation of the thickness mixing term in the form

$$\boldsymbol{u}_B = \frac{\overline{h'_\rho \mathbf{u}'_h}}{\bar{h}_\rho} = -\overline{\mathbf{u}'\frac{\partial}{\partial z}\left[\frac{\rho'}{\bar{\rho}_z}\right]} = -\left[\left(\frac{\overline{\rho'\mathbf{u}'}}{\bar{\rho}_z}\right)_z - \frac{\overline{\rho'\mathbf{u}'_z}}{\bar{\rho}_z}\right].$$

Assuming that density and velocity perturbations result from quasigeostrophic motion, thermal wind is a good approximation to the last term in the above expression so that

$$\overline{\rho'\mathbf{u}'_z} \approx -\frac{g}{\rho_0 f^2}\cdot \mathbf{f}\times\overline{\rho'\nabla_h\rho'} = -\frac{g}{\rho_0 f^2}\cdot \mathbf{f}\times\nabla_h\frac{1}{2}\overline{\rho'^2}.$$

In addition, a linearized equation of state leads to a simple approximation for the horizontal perturbation density flux; that is, $\overline{\mathbf{u}'\rho'} = \beta\overline{\mathbf{u}'S'} - \alpha\overline{\mathbf{u}'\Theta'}$. Using thermal wind and a linearized equation of state for the density perturbations, $\boldsymbol{u}_B$ then can be written as

$$\boldsymbol{u}_B \approx -\left[\left(\frac{\beta\overline{\mathbf{u}'S'}}{\bar{\rho}_z}\right)_z - \left(\frac{\alpha\overline{\mathbf{u}'\Theta'}}{\bar{\rho}_z}\right)_z + \frac{g}{\rho_0 f^2}\cdot\mathbf{f} \times\frac{1}{\bar{\rho}_z}\nabla_h\frac{1}{2}\overline{(\beta S' - \alpha\Theta')^2}\right];$$

$\overline{\mathbf{u}'\Theta'}$ could be calculated for all experiments. For experiments 2 and 3 we unfortunately had to infer $\overline{\mathbf{u}'S'}$ from a Θ–S relation because it was not summed up during the integration for all experiments. The contribution of the last term accounts for less than one percent of the signal and is therefore neglected. To calculate the mean correlations in the above expressions the data were averaged spatially and temporally.

GM90 parameterize the bolus velocity by adding a source term in the form of a divergence of mean thickness to the mean tracer advection equation. In level coordinates, this translates to a horizontal eddy-induced advection velocity $\mathbf{u}_{GM}$, given by

$$\mathbf{u}_{GM} = -(\kappa\mathbf{L})_z = -\kappa\mathbf{L}_z \text{ for constant } \kappa,$$

where

$$\mathbf{L} = -\left(\frac{\beta\nabla_h\bar{S} - \alpha\nabla_h\bar{\Theta}}{\beta\bar{S}_z - \alpha\bar{\Theta}_z}\right)$$

is a two-dimensional vector and κ is a parameter with dimensions of cm^2 s^{-1} describing the layer-thickness diffusivity. Here $\mathbf{L}$ points in the direction of increasing slope of the neutral surface with the slopes magnitude at its location and can easily be evaluated from the model data by calculating the mean Θ and S and using the model equation of state. Derivatives are calculated consistent with model numerics.

3. Data

The data used for our analysis were produced by the Cox–Bryan-type model (Bryan 1969; Cox 1984), which has been run at IfM Kiel in the CME configuration (Bryan and Holland 1989) with a resolution of $\frac{1}{3}° \times \frac{2}{5}°$ in the horizontal and 30 levels in the vertical. For detailed references on the model configuration and performance see, for example, Böning and Herrmann (1994).

We have chosen data from four independent model runs, which were all integrated over 5 years with one exception of 4 years, as can be seen from Table 1. Table 1 also contains some details about the forcing fields and boundary conditions that were used for the experiments. The data, that is, potential temperature, salinity,

TABLE 1. Overview of the 1/3° model runs. The horizontal Austausch coefficient for momentum (A_m) and the horizontal mixing coefficient (A_h) take values of -2.5×10^{19} cm^4 s^{-1}. Experiment 1 was forced by Hellerman and Rosenstein winds and experiments 2–4 were forced by Isemer and Hasse winds. The abbreviations are CE: Camp and Elsberry mixed layer, RL: restoring to Levitus in the northern boundary zone, RS: restoring toward a section in the northern boundary zone corrected for colder temperatures at depth relative to Levitus, LT, (ST): Mediterranean seawater restoring on a long (short) timescale.

	Experiment			
	1	2	3	4
Integral time	5	5	4	5
Mixed layer	—	—	CE	CE
Northern BC	RL	RL	RS	RS
Mediterranean BC	LT	LT	LT	ST

and the velocity components, as well as their correlations, were available in form of seasonal means, which were summed for each of the four experiments.

It turned out that the model integration time of 5 years was too short to calculate the statistical moments with sufficient accuracy. We believe, however, that it is legitimate to form averages over different experiments, as long as one stays away from regions directly influenced by changes in the boundary conditions between these experiments. Most of the data used in this work has been analyzed and discussed for diverse aspects in earlier articles (e.g., Stammer and Böning 1992; Böning and Herrmann 1994).

We will use only data in the region from 10° to 30°N, 20° to 60°W. The reason for choosing this region is twofold.

First, Stammer and Böning (1992) have shown in an intercomparison of model data and Geosat altimeter data that the model's mesoscale variability in this area is representative of the eddy kinetic energy level as derived from sea surface height variability. This is due to the model's ability in this region to resolve the first baroclinic Rossby radius of deformation as the dominant eddy scale, whereas north of 30°N the energy of the fluctuations is underestimated by the model by a factor of 2–10 (Treguier 1992). We therefore are confident that the model describes the observed variability fairly accurate in this region.

Second, the density field is, compared to other model areas, less influenced by the changes in boundary conditions.

A disadvantage however is that the eddy-induced tracer fluxes in this region are an order of magnitude smaller than in boundary current regions, which is one reason for the necessity of extensive averaging.

The southern part of this region is dominated by NEC dynamics with a strong seasonal cycle, which is however eliminated by annually averaging the seasonal averages. The turbulent fluxes, that is, $\overline{\mathbf{u}'\Theta'}$ and $\overline{\mathbf{u}'S'}$, which are used to calculate the eddy-induced advection velocity, are computed from seasonal averages before forming an annual average. Climatological monthly means that would result in an even better removal of the annual cycle were unfortunately not available.

A spatial scale analysis in form of a two-dimensional autocorrelation function determined that in order to calculate the first and second moments significantly, a spatial average over boxes of at least 2° × 2° is necessary. An error is estimated for each box average from standard deviations of temporal and spatial averaging. These errors are used as weights in a linear regression that gives an estimate for the mixing parameter κ.

4. Results

Table 2 shows correlation coefficients and error estimates for the horizontal components of the eddy-induced advection velocity $\boldsymbol{u}_B$ at levels 4–8 above the main thermocline. They are computed from spatially averaged data and are shown for an average over the four model experiments for each layer.

TABLE 2. Correlation coefficients $r_{u,v}$ and bolus velocity mean errors δu, v_B for the average over four experiments (1–4) for levels 4–8.

Depth (m)	r_u	r_v	δu_B (cm s^{-1})	δv_B (cm s^{-1})
133	0.50	0.55	0.007	0.016
180	0.72	0.35	0.008	0.017
233	0.85	0.66	0.008	0.014
295	0.94	0.72	0.006	0.013
370	0.82	0.84	0.002	0.046
Level 4–8	0.62	0.73	0.006	0.013

In the u component the correlation level varies only slightly after averaging over several experiments, while the correlation coefficients for the v component significantly increase in all levels with averaging period. An increase of the correlation coefficient for both components with depth is also found. The component-wise error estimates show a reduction of the error by more than 50% with a slightly decreasing tendency with depth. Estimates for the coefficient κ for each separate level vary unsystematically with depth. Therefore, an integral correlation and error for levels 4–8 are also given.

Figures 1a,b show scatter diagrams for the u and v component of the two representations of the eddy-induced advection velocities with the parameterization $\mathbb{L}_z$ as the abscissa, scaled with 1.0×10^7 in order to make both quantities comparable in magnitude and the bolus velocity $\boldsymbol{u}_B$ as the ordinate.

Shown is the data for levels 4–8 after averaging temporally over four experiments, giving an average over 19 years. Each dot then represents a spatial and temporal average in a 4° × 4° box on a single model level averaged over a period of 19 years. The correlation coefficients are 0.62 for the u and 0.73 for the v component. For the regression line the data are weighted with their relative error estimates in both variables. An estimate of the mean errors is given by the error bars shown in the lower right-hand corner of each figure.

The slope of the regression lines gives an integral estimate for the coefficient κ, resulting in $(1.11 \pm 0.5) \times 10^7$ cm^2 s^{-1} for the u component and $(0.67 \pm 0.5) \times 10^7$ cm^2 s^{-1} for the v component of $\mathbf{u}_{GM}$. Assuming systematic differences between both components, this translates into a value of $\kappa = (1.0 \pm 0.7) \times 10^7$ cm^2 s^{-1}.

We have unsuccessfully tried to obtain information on the spatial structure of the mixing coefficients by determining subregional correlation coefficients with varying box sizes. However, due to the high noise level, which is a consequence of only marginally satisfactory eddy statistics, no significant results could be obtained.

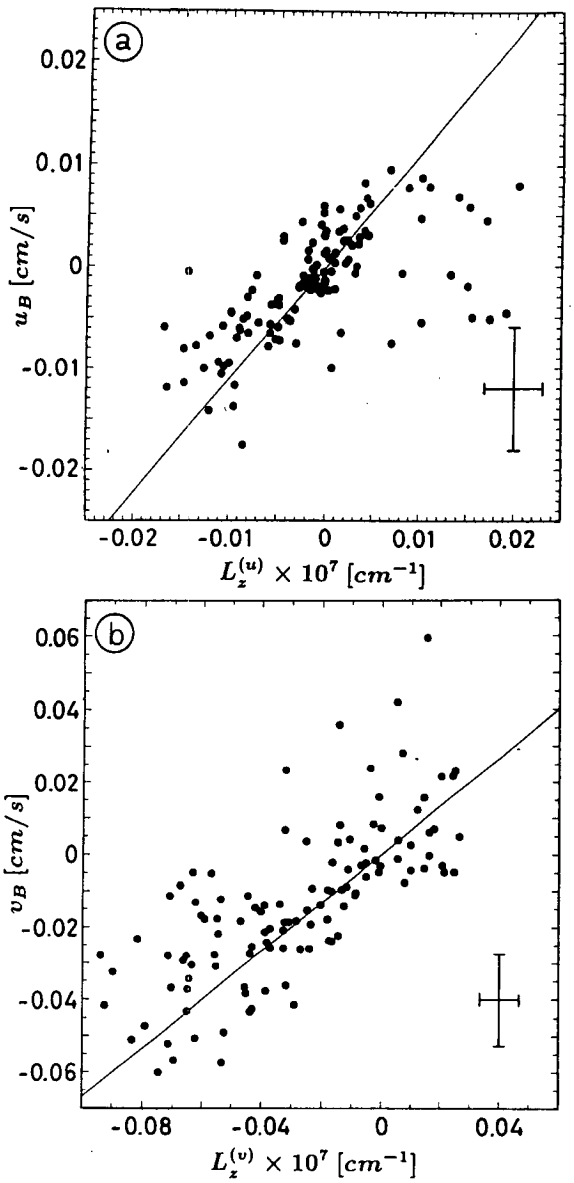

FIG. 1. Scatter diagram of the eddy-induced advection velocity versus its (scaled) parameterization $L_z \times 10^7$ in components for levels 4–8 (133–370 m). Each mark represents a 4° × 4° horizontal box and 19-yr time mean. The error bars show a mean value for deviations in both variables $(u, v)_{GM,B}$. The inclination of the regression line gives an estimate of the mixing parameter κ in 10^7 cm^2 s^{-1}. (a) Zonal component (in cm s^{-1}) and (b) meridional component (in cm s^{-1}) of the eddy-induced advection velocity and its parameterization. The resulting mixing parameters are $\kappa_u = (1.11 \pm 0.5) \times 10^7$ cm^2 s^{-1} for the u component and $\kappa_v = (0.70 \pm 0.5) \times 10^7$ cm^2 s^{-1} for the v component.

We have further attempted to directly represent the eddy heat and salt fluxes obtained from the model (more precisely the flux divergences) as a sum of the GM90 advective parameterization and of lateral mixing and formulated a simple inverse problem to estimate the respective parameters. Again, the noise level prevented an accurate determination of both parameters, and no information on their spatial or temporal structure could be obtained. Therefore, only the results of the regression analysis are presented.

5. Summary and conclusions

We have investigated the relationship between the horizontal component of the bolus velocity and its parameterization according to GM90 from data of a North Atlantic eddy-resolving circulation model. We have chosen to test the parameterization in a region south of 30°N where the model circulation compares favorably with observations and in particular simulates the mesoscale variability on a realistic energy level. We hence can expect to obtain a credible value for the thickness mixing parameter proposed by GM90.

It became evident that extensive averaging was necessary to find significant correlation between the eddy-induced advection velocity and its parameterization. This is so because the model integration times are too short to extract the signals beyond the noise level without further averaging.

We conclude that the layer thickness mixing parameterization as proposed by GM90 is not inconsistent with the mean horizontal tracer transport by mesoscale eddies above the main thermocline. The horizontal bolus velocity as calculated from the eddy-resolving model data show good correlation with the GM90 parameterization in the u and v components above the models main thermocline. An integral estimate of the mixing parameter κ yields values on the order of 10^7 cm^2 s^{-1}, which compare well to the numbers used in the coarse resolution experiments that were cited in the introduction. Our result as well as the improvements in these experiments support the view that a representation of the divergence of the turbulent tracer fluxes in the form of a diffusion–advection parameterization is a step toward a better tracer mixing parameterization in coarse-resolution models. We have estimated the layer thickness diffusivity as an average over a region of approximately 4000 km by 2000 km. As a consequence of the short integration times, no information about the spatial and temporal distribution of the mixing parameter κ could be obtained. An analysis of the spatial and temporal structure of mixing parameterizations will require costly long-term integrations. Improved resolution would be desirable, so that regions of boundary currents and higher latitudes can be included.

Acknowledgments. We are grateful to Dr. C. Böning for providing the model data and for helpful discussions. We would also like to thank Dr. A. M. Treguier for helpful remarks on performing isopycnal averages to calculate the bolus terms. Support by the German WOCE program, which is funded by the BMBF, is gratefully acknowledged.

REFERENCES

Böning, C. W., and R. G. Budich, 1992: Eddy dynamics in a primitive equation model: Sensitivity to horizontal resolution and friction. *J. Phys. Oceanogr.,* **22,** 361–381.

——, and P. Herrmann, 1994: Annual cycle of poleward heat transport in the ocean: Results from high-resolution modeling of the North and equatorial Atlantic. *J. Phys. Oceanogr.,* **24,** 91–107.

——, W. R. Holland, F. Bryan, G. Danabasoglu, and J. C. McWilliams, 1995: An overlooked problem in model simulations of the thermohaline circulation and heat transport in the Atlantic Ocean. *J. Climate,* **8,** 515–523.

Bryan, F., and W. R. Holland, 1989: A high-resolution simulation of the wind- and thermohaline-driven circulation in the North Atlantic Ocean. *Parameterization of Small-Scale Processes, Proc. Aha Huliko'a Hawaiian Winter Workshop,* Honolulu, HI, University of Hawaii, 99–115.

Bryan, K., 1969: A numerical method for the study of the circulation of the world ocean. *J. Comput. Phys.,* **4,** 347–376.

Cox, M. D., 1984: A primitive equation, three-dimensional model of the ocean. GFDL Ocean Group Tech. Rep. No. 1, GFDL Princeton University, 56 pp.

Danabasoglu, G., J. C. McWilliams, and P. R. Gent, 1994: The role of mesoscale tracer transports in the global ocean circulation. *Science,* **264,** 1123–1126.

Gent, P. R., and J. C. McWilliams, 1990: Isopycnic mixing in ocean circulation models. *J. Phys. Oceanogr.,* **20,** 150–155.

——, J. Willebrand, T. J. McDougall, and J. C. McWilliams, 1995: Parameterizing eddy-induced tracer transports in ocean circulation models. *J. Phys. Oceanogr.,* **25,** 463–474.

Hellerman, S., and M. Rosenstein, 1983: Normal monthly wind stress over the world ocean with error estimates. *J. Phys. Oceanogr.,* **13,** 1093–1104.

Isemer, H.-J., and L. Hasse, 1987: *The Bunker Climate Atlas of the North Atlantic Ocean.* Vol. 2. *Air–Sea Interactions,* Springer-Verlag, 252 pp.

McDougall, T. J., 1991: Parameterizing mixing in inverse models. *Dynamics of Oceanic Internal Gravity Waves, Proc. Aha Huliko'a Hawaiian Winter Workshop,* P. Müller and D. Henderson, Eds., Honululu, HI, University of Hawaii, 355–386.

Redi, M. H., 1982: Oceanic isopycnal mixing by coordinate rotation. *J. Phys. Oceanogr.,* **12,** 87–94.

Rhines, P. B., 1986: Lectures on ocean circulation dynamics. *Large Scale Transport Processes in Oceans and Atmosphere,* J. Willebrand and D. L. T. Anderson, Eds., ASI Series C190, Reidel, 105–161.

Stammer, D., and C. W. Böning, 1992: Mesoscale variability in the North Atlantic Ocean from GEOSAT altimetry and WOCE high-resolution, numerical modeling. *J. Phys. Oceanogr.,* **22,** 732–752.

Treguier, A. M., 1992: Kinetic energy analysis of an eddy-resolving, primitive equation model of the North Atlantic. *J. Geophys. Res.,* **97,** 687–701.